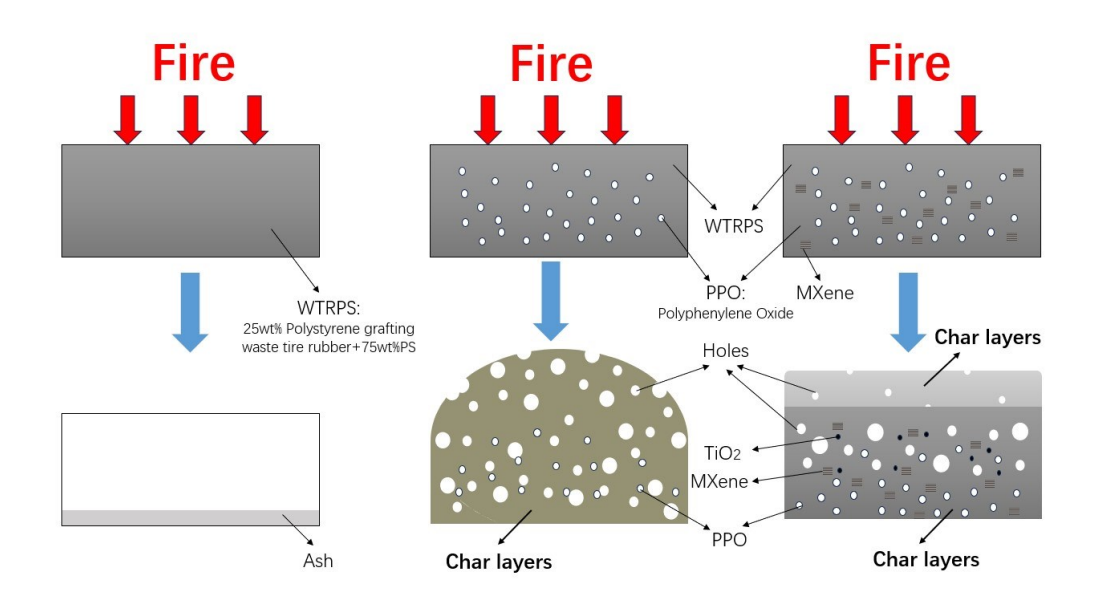
# Synergistic Flame Retardancy of MXene and Poly(*p*-Phenylene Oxide) on High-Performance Recycling Waste Rubber Modified Polystyrene Composites

Aoxue Tian,<sup>a</sup> Jinlong Zhang,<sup>b,c,\*</sup> and Yong Wang <sup>a,\*</sup>

\* Corresponding authors: jinlongzhang914@gmail.com; wangyong79@wust.edu.cn

DOI: 10.15376/biores.20.3.7713-7727

#### **GRAPHICAL ABSTRACT**



# Synergistic Flame Retardancy of MXene and Poly(*p*-Phenylene Oxide) on High-Performance Recycling Waste Rubber Modified Polystyrene Composites

Aoxue Tian, Iinlong Zhang, b,c,\* and Yong Wang a,\*

The development of high-performance polystyrene composites modified with recycling waste tire rubbers composed of natural and synthetic rubber mixture is highly desirable for a sustainable society. To tackle the intrinsic fire issue of waste tire rubber and polystyrene (WTRPS) composites for its advanced applications, the synergistic effect of fire additives MXene and poly(p-phenylene oxide) PPO on the performance of WTRPS composites was investigated in this work. The limited oxygen index values of WTRPS composites with MXene and PPO loading at 15 and 40 wt% were increased to 23.0%, compared to that of WTRPS at 17.0%. Additionally, the heat release rate, total heat release, and peak of heat release rate of resulting composites showed obvious decreases, confirming their synergistic fire retardancy effects on WTRPS composites. The synergistic mechanism was based on the char effect of PPO, heat sink effect of MXene, and catalyst effect of titanium dioxide generated from MXene. The synergistic strategy in this work paves a new avenue to develop fire retarding bio-composites of wood flour reinforced polyhydroxyalkanoates along with environmentally friendly fire additives (e.g., MXene and lignin or phytic acid) for advanced applications.

DOI: 10.15376/biores.20.3.7713-7727

Keywords: Waste tires; Recycling; Fire retardancy; MXene; Poly(p-phenylene oxide)

Contact information: a: College of Resources and Environment Engineering, Wuhan University of Science and Technology, Wuhan, 430081, PR China; b: State Key Lab of Metastable Materials Science and Technology, College of Materials Science and Engineering, Yanshan University, Qinhuangdao, 066004, China; c: School for Engineering of Matter, Transport and Energy, Arizona State University, Tempe, AZ 85287, USA; \*Corresponding authors: jinlongzhang914@gmail.com; wangyong79@wust.edu.cn

#### INTRODUCTION

Polystyrene (PS), one of the widely used thermoplastics, possesses excellent properties, such as excellent processability and good dielectric properties, while its low impact strength restricts diverse applications. To tackle its low impact strength, in the previous article, the surface grafting modification of waste tire rubber and polystyrene (WTRPS) composites with enhanced impact strength at about 4 times was reported (Tian et al. 2024). For its advanced applications, low fire retarding performance as another issue needs to be further addressed. As both components of WTRPS composites are organic materials and easily ignited, the limited oxygen index (LOI) value of PS is around 18.0%, and its intrinsic high flammability during combustion further restricts its advanced applications (Li et al. 2020). Therefore, it is imperative to improve the WTRPS composite flame retardancy.

In terms of fire retarding properties of WTRPS composite materials, there have been few reports, except for studies about waste tire rubber modified ethylene-vinyl acetate EVA and polyurethane foam composites (Wiśniewska et al. 2023, 2024; Zhang et al. 2023; Hejna et al. 2024). Most studies have focused on fire retardancy of pure PS resin and its foam materials. For instance, phosphorus- and nitrogen-based flame retardants were widely explored in PS fire retardancy (Chigwada and Wilkie 2003). Unfortunately, PS composites usually had a limited fire retarding enhancement. Additionally, ammonium polyphosphate and magnesium hydroxide as additive-type fire retardants have been widely studied to endow PS with improved flame retardancy. However, because of the deterioration of miscibility, the high loading of these fire additives resulted in the PS composites with low flame retardancy durability due to fire additives leaching from PS matrix. Fortunately, poly(p-phenylene oxide) (PPO) as an engineering plastic is miscible with PS at almost any ratio, and it is also an excellent flame retardant by the formation of carbon chars during its combustion, which is called the char effect. Additionally, the high molecular weight nature of PPO prevents its leaching from the PS matrix. However, PPO alone usually can't achieve a satisfying performance in fire retardancy of PS. For example, the LOI value of PPO/PS composites achieved around 21.0% (Tuan et al. 2024). To further enhance PS fire retardancy, it is a good idea to combine with other fire retardants to achieve synergistic fire retardancy.

As a novel 2D material with a unique structure and transition metal element, MXene in flake nanosheet structures sounds like a promising fire additive to further tailor flame retardancy of PS. Inspired by the previous fire retardant nanoclay, the fire retarding mechanism of MXene is primarily based on the so-called "tortuous path" barrier effect that is expected to inhibit mass and heat exchange among solid and gas phase. Additionally, various types of titanium dioxides (TiO<sub>2</sub>) generated during the MXene decomposition contribute to the catalyst effect (He *et al.* 2019; Liu *et al.* 2023; Mao *et al.* 2023). However, the application of PPO and MXene as synergistic flame retardants of WTRPS composites has not been reported yet, and its synergistic fire retarding mechanism is also not clearly known. Thus, it was hypothesized that the presence of MXene along with PPO might be expected to contribute to a high-performing char layer of WTRPS composites when exposed to flame.

Herein, the fire retarding performance of polystyrene grafting waste tire rubber and PS composites with fire additives PPO and MXene was investigated *via* the limited oxygen index test. To mimic the real fire scenario, the cone calorimetry test was further studied on composite materials. Besides, according to the char residual morphology and chemical structure analysis, the flame retarding mechanism was proposed. The synergistic strategy in this work is promising for fire retarding bio-composites of wood flour reinforced polyhydroxyalkanoates (Zhang *et al.* 2017; Vandi *et al.* 2018) and cellulose aerogels (Zhang *et al.* 2024).

#### **EXPERIMENTAL**

#### **Materials**

The PS resin was received from Zhanjiang Xinzhongmei Chemical Co. Polystyrene grafting waste tire rubber was prepared according to the authors' previous publication (Tian *et al.* 2024). MXene (Ti<sub>3</sub>C<sub>2</sub>, black powers with particle size of 10 μm) and PPO (white pellets with melt flow index of 10g/10min and molecular weight of 30,000 to 60,000

g/mol) were purchased from Hesimo New Materials Technology Co and Shabo Jichu Innova Plastics Co., respectively.

### **Melting Compounding of BWTRPS and WTRPS Composites**

The weight ratio of polystyrene grafting waste tire rubber (or bare waste tire rubber) and PS was maintained at 25/75. PPO loading was kept at 20 and 40 wt%, and MXene at various contents from 5 to 30 wt% was introduced into the WTRPS composites. Table 1 lists the component contents and names of all the blends. BWTRPS and WTRPS denote 25 wt% bare waste tire rubber/PS composites and 25 wt% polystyrene grafted waste tire rubber/PS composites; WTRPS/PX (X = 20 or 40) means 25 wt% polystyrene grafted waste tire rubber/PS composites with PPO loading at 20 and 40 wt%; WTRPS/PX/MY (Y = 5, 15, and 30) represents 25 wt% polystyrene grafted waste tire rubber/PS composites with fire additives PPO content at 40 wt% and MXene content at 5, 15, and 30 wt%.

**Table 1.** Component Contents and Abbreviations of BWTRPS and WTRPS Composites

Samples	PPO	MXene
BWTRPS	0	0
WTRPS	0	0
WTRPS/P20	20	0
WTRPS/P40	40	0
WTRPS/P40/M5	40	5
WTRPS/P40/M15	40	15
WTRPS/P40/M30	40	30

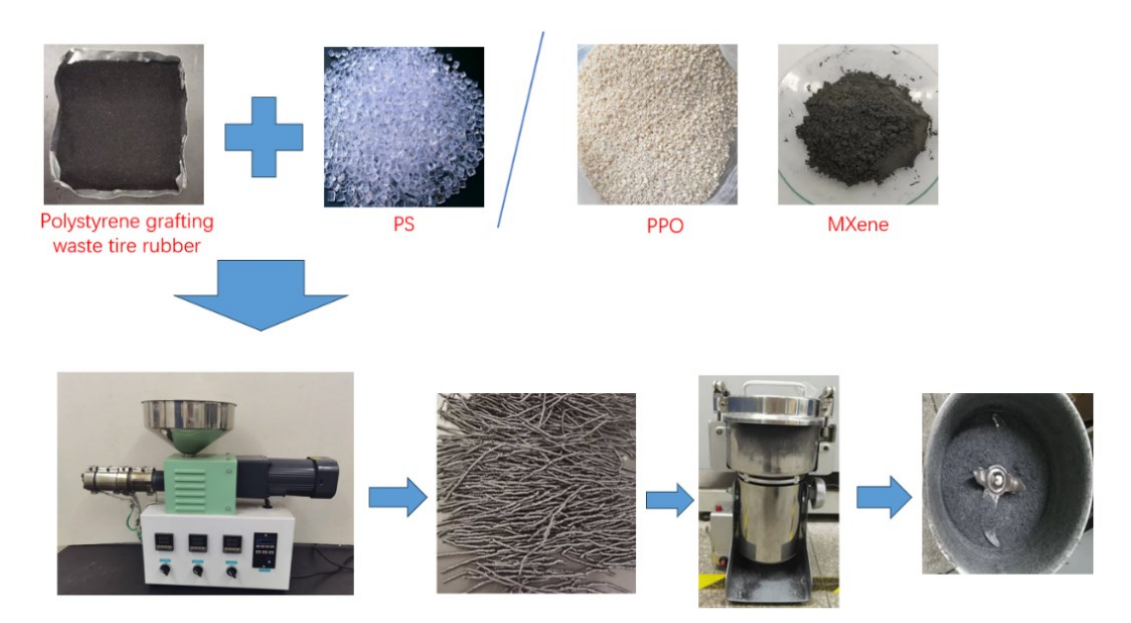


Fig. 1. Scheme of preparation of WTRPS and WTRPS/P/M composites

The PS, polystyrene grafting waste tire rubber (or bare waste tire rubber), PPO and/or MXene blends were melt-extruded between 160 and 290 °C *via* a single screw extruder (R77F-NA50-112B5, Wuhan Weier Plastic Machinery Co.), as shown in Fig. 1. The extrusion temperature was closely dependent on PPO loading. The extruded samples were then granulated for compounding tensile and impact standard samples with a designed

mold *via* hot-press compounding (QLB-25D/Q, Jiangsu Xinzhenwei Experiment Machinery Co.). For the composite sheet preparation in fire retarding test, the pellets of melting blends were compounded *via* hot-press (QLB-25D/Q, Jiangsu Xinzhenwei Experiment Machinery Co.) at 250 °C to form the 4 mm thick sheets.

#### Fire, Residue, and Mechanical Characterization

LOI values of WTRPS, WTRPS/P, and WTRPS/P/M composites were measured using a limited oxygen index tester (Suzhou Yangyi Woerqi Detection Technology Co.) according to the test procedure of GB/T2406. Fire performance of WTRPS, WTRPS/P, and WTRPS/P/M composites was further measured with a cone calorimeter (Firemana Safety Technology Co.) according to the GB/T 16172 standard using 100 mm × 100 mm test samples. The composite samples were exposed to heat radiation of 25 kW/m<sup>2</sup>. The top sample surface morphology was taken with a digital camera after the combustion test. The char residues of WTRPS, WTRPS/P, and WTRPS/P/M via SEM (Nova 400Nano, Philips Electron Optics) were sputtered with gold before measurement. The X-ray diffraction (D/MAX-2500/PC, Rigaku) and Raman spectroscopy (E55+FRA106, Bruker) along with X-ray photoelectron spectroscopy (XPS, AXIS SUPRA+, NULL) were used to characterize the char residue of WTRPS, WTRPS/P, and WTRPS/P/M composites. The volatiles released during combustion of WTRPS and WTRPS/P/M composites were tested by thermogravimetric analysis-infrared spectrometry (TG-IR, TGA8000-Spectrum3, PerkinElmer) from ambient temperature to 800 °C at a scanning rate of 20 °C/min in nitrogen atmosphere. The flexural strength of PS, WTRPS, WTRPS/P, and WTRPS/P/M composites was tested using a universal testing machine (WDW-100D, Jinan Chuanbai Instrument Equipment Co., Jinan, China) according to GB/T 9341 (2008). The testing rate was 2 mm/min. The length, width, and thickness of the sample were  $80 \pm 2$  mm,  $10.0 \pm 0.2$ mm, and  $4.0 \pm 0.2$  mm, and the sample span was 64 mm. The impact strength of PS, WTRPS, WTRPS/P, and WTRPS/P/M composites was measured by an impact machine (ZWJ-0350, Jiangdu Xinzhenwei Testing Machinery Co., Jiangdu, China) according to GB/T 1043 (2008).

#### **RESULTS AND DISCUSSION**

### Fire Retarding Properties

Limited oxygen index test

The LOI data of PS, BWTRPS, WTRPS, WTRPS/P, and WTRPS/P/M composites are listed in Table 2. The neat PS, BWTRPS, and WTRPS exhibited LOI values of 18.0% (Li *et al.* 2020), 17.0%, and 17.0%. The addition of PPO at 40 wt% significantly enhanced the LOI value at 21.1% of WTRPS/P40 compared with those of pure PS and WTRPS at 18.0 and 17.0%, which can be attributed to its char layer effect. Namely, during the fire propagation, these char layers worked as an insulating barrier, which mitigated flammable gas diffusion and heat exchange among flame areas and WTRPS composite substrates, thereby slowing down and/or terminating its further pyrolysis. However, most of WTRPS composites were already combusted, as PPO had a relatively higher thermal degradation temperature at around 440 °C and was hard to produce an effective char layer at the early combustion stage. Therefore, pure PPO at even 40 wt% loading still couldn't achieve a satisfactory fire retarding performance. Most importantly, the addition of fire additive MXene further improved the LOI values of the WTRPS/P/M composites. Especially, the

LOI values of WTRP/P/M composites with MXene loading at 15 and 30 wt% reached 23.0 and 24.1%, respectively. The enhanced flame retardancy was attributed to the synergistic dense char layer of PPO, the tortuous barrier path and heat sink effect of MXene sheets, and catalyst effect of TiO<sub>2</sub> produced during its decomposition.

**Table 2.** LOI Values of PS, BWTRPS, WTRPS, WTRPS/P, and WTRPS/P/M Composites

Samples	LOI (%)	
PS	18.0 (Li et al. 2020)	
BWTRPS	17.0	
WTRPS	17.0	
WTRPS/P20	18.7	
WTRPS/P40	21.1	
WTRPS/P40/M5	21.7	
WTRPS/P40/M15	23.0	
WTRPS/P40/M30	24.1	

The residual morphology of BWTRPS, WTRPS, WTRPS/P, and WTRPS/P/M composites after the LOI test is shown in Fig. 2.



**Fig. 2.** Char morphology of BWTRPS, WTRPS, WTRPS/P, and WTRPS/P/M composites with LOI test (a: BWTRPS, b: WTRPS, c: WTRPS/P25, d: WTRPS/P40, e: WTRPS/P40/M5, f: WTRPS/P40/M15, and g: WTRPS/P40/M30)

For the BWTRPS and WTRPS composite samples, no char layers were observed, while WTRPS/P composite samples established obviously intumescent char layers, especially at 40 wt% PPO loading. For WTRP/P/M composite samples, dense char layers were produced, especially in WTRP/P40/M15 and WTRP/P40/M30 composites, which support the obviously enhanced LOI values of WTRP/P40/M15 and WTRP/P40/M30 composites at 23.0 and 24.1%. However, 30 wt% MXene loading was relatively high for maintaining overall performance of resulting composites in its advanced applications. Therefore, the WTRPS, WTRPS/P40, and WTRPS/P40/M15 composites as representatives were studied further in cone calorimetry and fire retarding mechanism.

#### Cone calorimetry test

The combustion parameters in terms of total heat release (THR), heat release rate (HRR), HRR peak (pHRR), and mass loss (ML) of WTRPS, WTRPS/P40, and WTRPS/P40/M15 composites are shown in Fig. 3(a-c). According to Fig. 3a and Table 3, all samples had one pHRR, which appeared in the range of 12 and 600 s. The WTRPS composites displayed the highest pHRR of 737.4 kW/m² at 200 s, and WTRPS/P40/M15 composites had the lowest pHRR of 367.6 KW/m² at 300 s. Additionally, the retarding of ignition time of WTRPS/P40/M15 composites to 53 s was observed compared to these of WTRPS composites at 12 s and WTRPS/P40 composites at 49 s.

**Table 3.** Fire Retarding Properties of WTRPS, WTRPS/P40, and WTRPS/P40/M15 Composites

Samples	Ignition Time	THR (MJ•m <sup>-2</sup> )	pHRR (kW•m <sup>-2</sup> )
WTRPS	12	148.9	737.4
WTRPS/P40	49	145.1	494.6
WTRPS/P40/M15	53	111.0	367.6

For WTRPS/P40 composites, the decrease of HRR, pHRR, and THR values was clearly observed compared to these of the WTRPS composites. The addition of PPO also obviously reduced the mass loss (ML) values, as shown in Fig. 3c.

The improvement of fire performance in WTRPS/P40 composites was attributed to the formation of char layers after its degradation of fire additive PPO, which act as an effective barrier preventing WTRPS substrates from further combustion. For WTRPS/P40/M15 composites, HRR, THR, and pHRR values decreased further compared to both WTRPS/P40 and WTRPS composites, indicating the synergistic effect of fire additives MXene and PPO.

Additionally, the combined use of MXene and PPO showed an even better fire retardancy with a slightly further reducing ML values. The MXene platelet barrier effect blocked the heat and mass transfer along with the catalyst effect of TiO<sub>2</sub>. Namely, the TiO<sub>2</sub> released from MXene further removed the high energy heat in the gas phase, which mitigated the pyrolysis of the WTRPS composite substrates and retarded mass losses and energy release rates of their decomposed products. These results indicated the synergistic effect of MXene and PPO on flame retardancy of WTRPS. The cone calorimetry results had a good match with LOI results in Table 2.

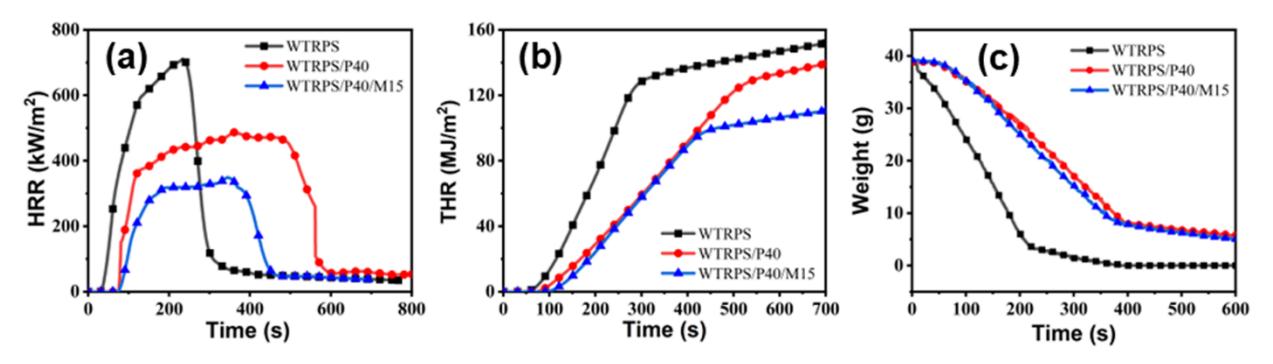


**Fig. 3.** Heat release rate (a), mass loss (b), and total heat release (c) of WTRPS, WTRPS/P40, and WTRPS/P40/M15 composites under cone calorimetry test

## **Char Residual Morphology**

Char residue morphology after the cone calorimetry test of WTRPS, WTRPS/P40, and WTRPS/P40/M15 composites are shown in Fig. 4. The sample surface was burnt out in some areas for the WTRPS composite sample (Fig. 4a), indicating poor fire retardancy performance. For the WTRPS/P40 composite sample (Fig. 4b), continuous char layers were observed, but the char residues had holes and cracks. However, for char residues of WTRPS/P40/M15 composite sample (Fig. 4c), continuous and compact char layers were generated, indicating the synergistic effect of MXene and PPO on fire retardancy of WTRPS.

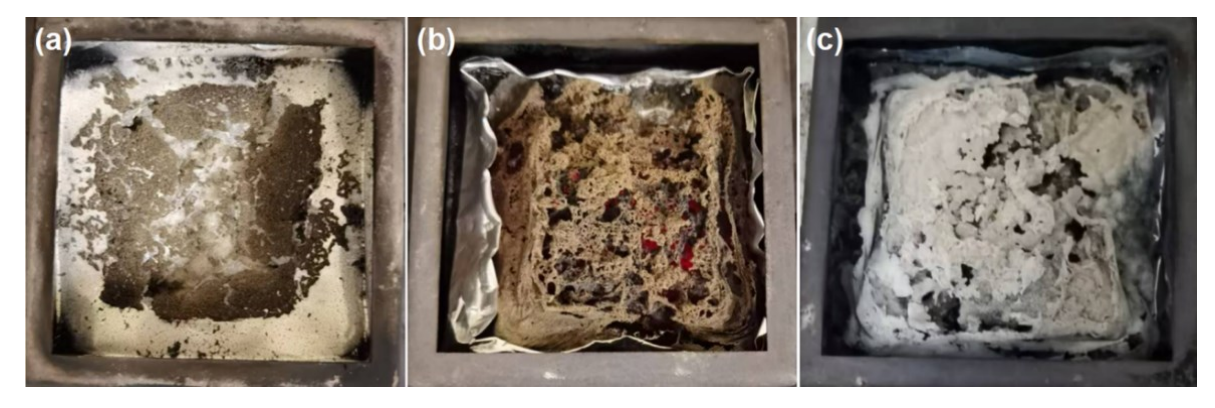
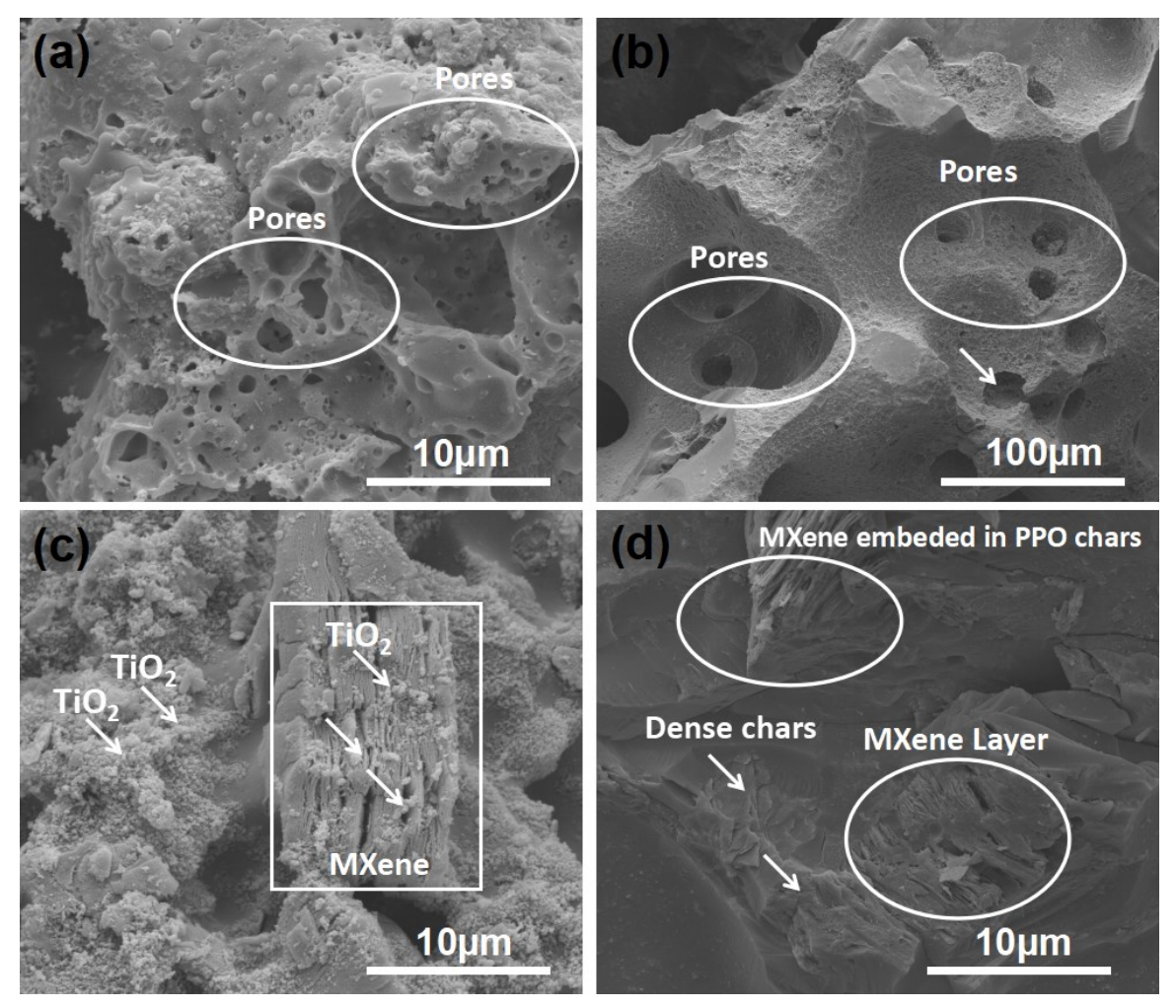


Fig. 4. Char residues of WTRPS (a), WTRPS/P40 (b), and WTRPS/P40/M15 (c)

The SEM images of char residues of WTRPS, WTRPS/P40, and WTRPS/P40/M15 composites are shown in Fig. 5. For WTRPS (Fig. 5a), many large holes were clearly apparent on the char residual surface, which contributed to the fast gas diffusion and heat transfer. Thus, WTRPS burnt up quickly. For the char residues of WTRPS/P40 composites (Fig. 5b), small holes on char layer surfaces were found as the char layers were weak, and combustion gases broke unstable char layers. This structure had a certain fire retardancy on WTRPS matrix, but it is hard to establish an effective flame retardancy. As a contrast, continuous and compact char layers were observed in WTRPS/P40/M15 composites (Fig. 5c), thereby governing the enhanced fire retardancy. The above morphology supported the synergistic effect of MXene and PPO, again.



**Fig. 5.** SEM images of char residues of WTRPS (a), WTRPS/P40 (b), and WTRPS/P40/M15 composites (c-d)

#### **Char Residual Structure**

X-ray diffraction (XRD), XPS, and Raman spectroscopy measurements (Fig. 6a-d) were conducted to further understand the char residual structure and chemical composition. According to Fig. 6a, no characteristic peaks were observed in WTRPS/P40 composites, while the characteristic peaks at (101), (004), (200), and (105) were clearly apparent in WTRPS/P40/M15 composites, which corresponded to the anatase phase of titanium dioxide (TiO<sub>2</sub>).

According to the XPS spectra in Fig. 6b, regarding the char residues of WTRPS/P40/M15 composites, Ti, C, and O elements were clearly observed, while only O and C elements were detected about char residues of WTRPS and WTRPS40 composites. According to the high resolution XPS spectrum of WTRPS/P40/M15 composites in Fig. 6c, the Ti 2p spectrum had two characteristic peaks, which were related to Ti 2p<sub>3/2</sub> and Ti 2p<sub>1/2</sub>, further confirming the generation of TiO<sub>2</sub>. These results indicated TiO<sub>2</sub> particles were produced from MXene during the combustion, which had a good match with SEM images in Fig. 5(c-d) regarding the presence of TiO<sub>2</sub> particles.

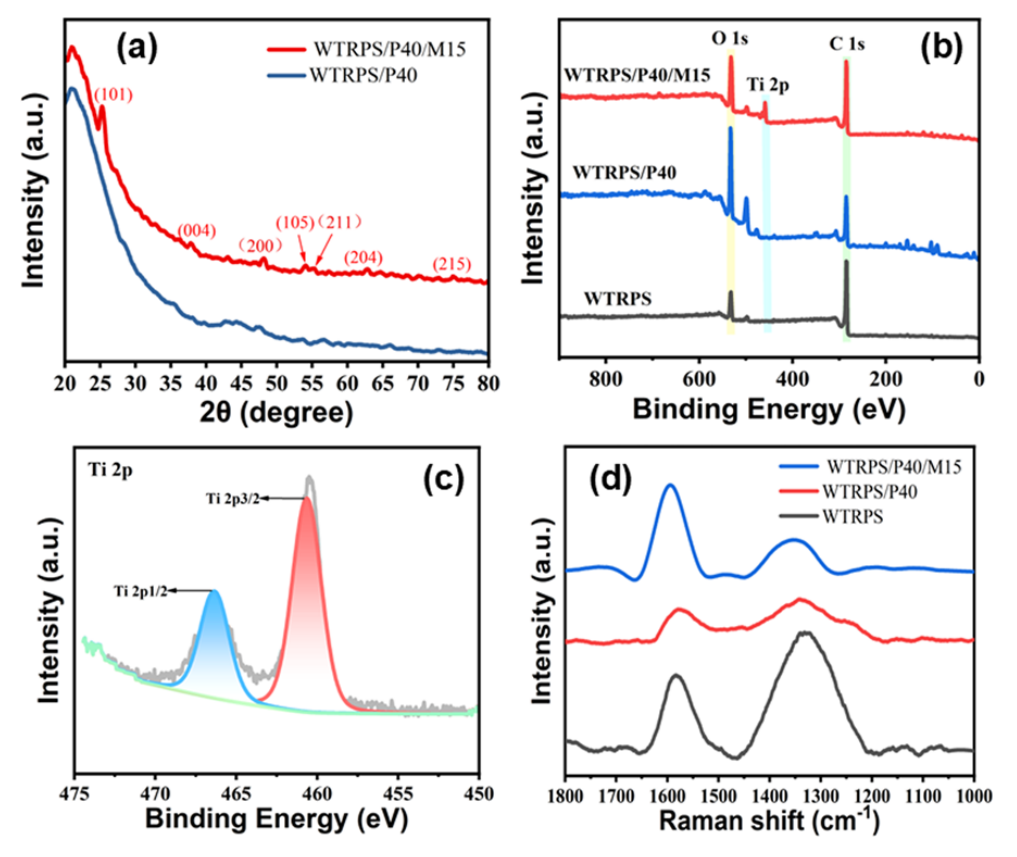


**Fig. 6.** XRD patterns of WTRPS/P40 and WTRPS/P40/M15 composites (a) and XPS and Raman spectra of WTRPS, WTRPS/P40, and WTRPS/P40/M15 composites (b-d): Char residues after cone calorimeter tests

Additionally, the charred quality is affected by the graphitic carbon content, which determines fire retarding performance. According to Raman spectra in Fig. 6d, two typical peaks at 1350 (called D band) and 1580 cm<sup>-1</sup> (called G band) were clearly observed, which corresponded to the disordered graphite or glass carbons. The intensity ratio of D band to G band ( $I_D/I_G$ ) defines the graphitization degree of char residues. The  $I_D/I_G$  value ( $I_D/I_G = 0.85$ ) of WTRPS/P40/M15 composites was slightly decreased compared to those of WTRPS/P40 ( $I_D/I_G = 1.08$ ) and WTRPS composites ( $I_D/I_G = 1.18$ ), indicating the increase of graphitization degree with the synergistic effect of PPO and MXene. These results further confirmed the synergistic fire retardancy of PPO and MXene on WTRPS composites. Additionally, according to the TG-IR spectra (Fig. S1), the volatiles released during combustion of WTRPS/P40/M15 composites were reduced obviously compared to WTRPS composites, which also supported PPO and MXene as effective fire additives for WTRPS composites.

# **Proposed Fire Retarding Mechanism and Potential Extension Applications**

The synergistic fire retarding mechanism of MXene and PPO is proposed in Fig. 7. For WTRPS composites, both waste tire rubber and PS are flammable materials and easily fired (namely, the LOI value with less than 21). For WTRPS/P40 composites, PPO was decomposed into char layers at around 430 °C (Lombardi et al. 2012) and then displayed fire retardancy for WTRPS matrix. But its char layers were easily broken by the combustion free radicals and then formed holes on its char layer surfaces. Meanwhile, at

temperature below 400 °C, WTRPS matrix was combusted quickly as PPO fire additives had no decomposition to establish char layers for retarding flame of WTRPS matrix. Therefore, PPO contributed a certain amount of fire retardancy to the WTRPS matrix. For WTRPS/P40/M15 composites, MXene decomposed to produce TiO2 around 300 °C (Hai et al. 2020). Therefore, TiO2 as a radical scavenger captured free radicals generated from the WTRPS matrix. As a result, MXene retarded the flame of WTRPS matrix. Additionally, TiO2 worked as a catalyst to promote the decomposition of PPO early (He et al. 2019), and then PPO could establish effective residual char layers covering on the surface of WTRPS matrix. The robust hybrid char layers of PPO and MXene worked as effective insulation layers for WTRPS matrix during combustion. Based on the synergistic effects, namely, PPO char effect and barrier and heat sink effect of MXene, they established an excellent fire retardancy for WTRPS matrix.

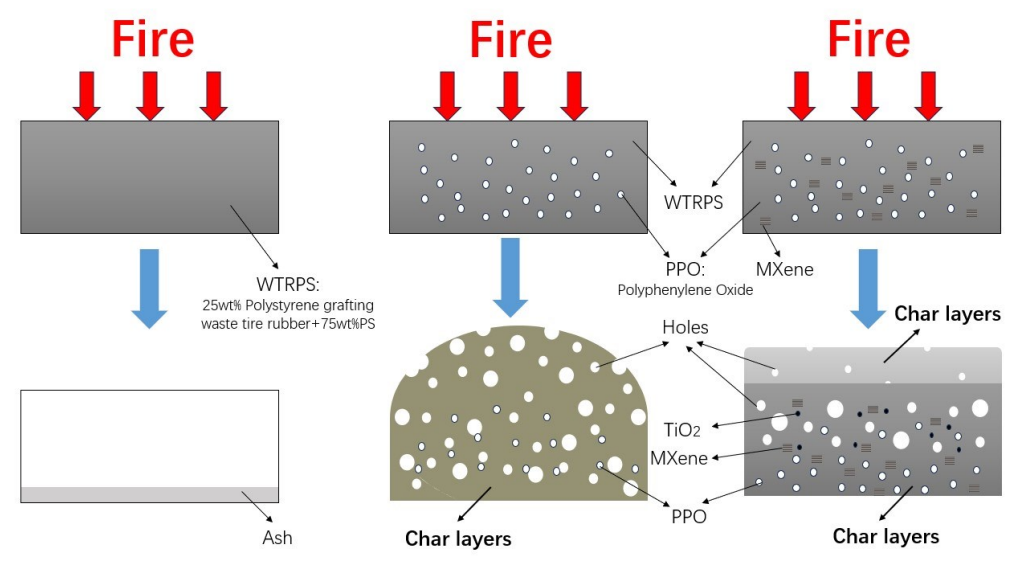
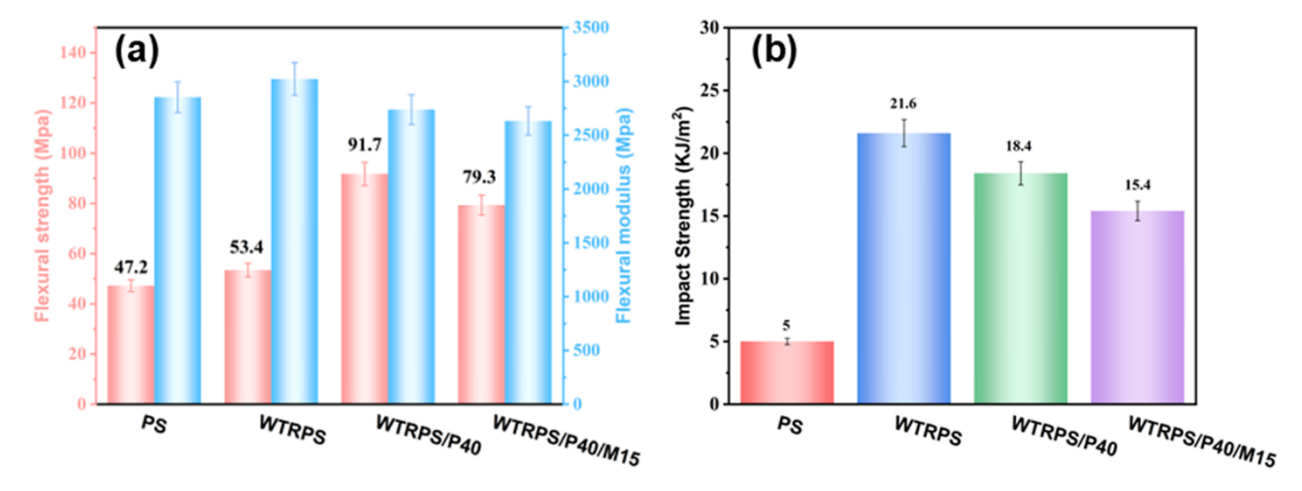


Fig. 7. Scheme of proposed fire retarding mechanism of MXene and PPO on WTRPS composites

The synergistic fire additives MXene and PPO showed their potential for fire retardancy of wood flour and plastic composites (WPC) and wood-based composites (e.g., plywood and lumbers) via lamination coating for a broad application (Hosseinashrafi et al. 2023). In a previous study, the synergistic fire additives 1,2-bis(pentabromophenyl) and nanoclay displayed excellent flame retarding performance on WPC (Zhang et al. 2017). As both clay and MXene have a similar platelet structure, the synergistic MXene and PPO fire retarding system probably also works for WPC. Additionally, MXene and PPO fire additives have a large chance of conveying fire retardancy to wood-based composites via the lamination coating, namely, sandwich structures with the MXene and PPO composite sheets as the top and bottom layers and plywood or lumbers as the middle layer followed by the hot press. It is also possible for fire retarding biodegradable polymers via this lamination coating strategy, such as polylactide or polylactide/nanocellulose biocomposites. Besides, MXene and graphene are both layered structure, and graphene as the fire additives or synergistic components has been studied for fire retarding polymer composites (Sang et al. 2016). Owing to the relatively high price of MXene as fire retarding fillers, searching for its alternative is also an interesting topic. Therefore, wood-sourced graphene as an alternative to MXene has potential for fire retarding WPC and wood-based composites (Severo et al. 2021), which is highly desirable for future research.

# **Mechanical Properties**

The mechanical properties of neat PS, WTRPS, WTRPS/P40, and WTRPS/P40/M15 composites are shown in Fig. 8 (a-b). The impact strength of WTRPS composites had increased almost 4 times compared to pure PS (Fig. 8b), indicating the enhanced interfacial adhesive of PS and waste tire rubber *via* its surface modification by styrene under conventional free radical polymerization, while WTRPS/P40 and WTRPS/P40/M15 composites with the addition of fire additives PPO and/or MXene had slight reduction from 21.6 kJ/m² to 18.4 and 15.4 kJ/m², respectively. Additionally, compared to WTRPS composites, the flexural strength of WTRPS/P40 and WTRPS/P40/M15 composites increased from 53.4 MPa to 91.7 and 79.3 MPa (Fig. 8a), respectively, while the flexural modulus of PS, and WTRPS, WTRPS/P40 and WTRPS/P40/M15 composites almost showed no obvious changes (Fig. 8a), which followed the tendency in literature (Sartore *et al.* 2006). These results indicated that the WTRPS/P40/M15 composites still maintained decent mechanical performance with the addition of fire additives PPO and MXene.



**Fig. 8**. Flexural strength and modulus (a) and impact strength (b) of PS, WTRPS, WTRPS/P40 and WTRPS/P40/M15 composites

#### CONCLUSIONS

- 1. The lower oxygen index (LOI) values of waste tire rubber, polystyrene and MXene (WTRP/P/M) composites with MXene loading at 15 and 30 wt.% reached 23.0 and 24.1% compared to that of WTRPS composites at 17.0%, which had an obviously enhanced fire retardancy.
- 2. The total heat release (THR), peak of heat release rate (pHRR), and mass loss (ML) of WTRPS/P40/M15 composites had an obvious decrease compared to those of WTRPS and WTRPS/P40 composites, indicating the synergistic fire retardancy of poly(p-phenylene oxide) (PPO) and MXene.
- 3. Continuous and dense char layers were generated in terms of WTRPS/P40/M15 composites according to scanning electron microscope (SEM) images, confirming the synergistic fire retardancy of fire additives MXene and PPO.
- 4. The synergistic fire retardancy mechanism was based on the hybrid char layers of PPO and MXene along with the heat sink effect and catalyst effect of TiO<sub>2</sub>.

#### **ACKNOWLEDGMENTS**

The authors are grateful for the support of the Natural Science Foundation of Hebei Province (Grant No. E2020203063) and Department of Education Foundation of Hebei Province (Grant No. QN2020104). The authors acknowledge the use of facilities from Prof. Hongxiang Chen's lab in College of Chemistry and Chemical Engineering at Wuhan University of Science and Technology, China. The authors also acknowledge Prof. Kun Zhai from State Key Lab of Metastable Materials Science and Technology, College of Materials Science and Engineering at Yanshan University, China regarding Raman spectrum and X-ray diffraction measurements.

#### REFERENCES CITED

- Chigwada, G., and Wilkie, C. A. (2003). "Synergy between conventional phosphorus fire retardants and organically-modified clays can lead to fire retardancy of styrenics," *Polym. Degrad. Stability* 81, 551-557. DOI: 10.1016/S0141-3910(03)00156-3
- Hai, Y., Jiang, S. H., and Niu, S. H. (2020). "Fire-safe unsaturated polyester resin nanocomposites based on MAX and MXene: A comparative investigation of their properties and mechanism of fire retardancy," *Dalton Trans* 49, article 5803. DOI: 10.1039/d0dt00686f
- He, L. X., Wang, J. L., Wang, B. B., Wang, X., Zhou, X., Cai, W., Mu, X. W., Hou, Y. B., Hu, Y., and Song, L. (2019). "Large-scale production of simultaneously exfoliated and Functionalized Mxenes as promising flame retardant for polyurethane," *Composites Part B* 179, article ID 107486. DOI: 10.1016/j.compositesb.2019.107486
- Hejna, A., Kosmela, P., Olszewski, A., and Żukowska, W. (2024). "The input of nanoclays to the synergistic flammability reduction in flexible foamed polyurethane/ground tire rubber composites," *Materials* 17(21), article 5344. DOI: 10.3390/ma17215344
- Hosseinashrafi, S. K., Hosseinihashemi, S. K., Gorji, P., and Akhtari, M. (2023). "Environment-friendly waterborne fire retardants for protection of wood and bark against fire flames," *BioResources* 18(4), 7681-7699. DOI: 10.15376/biores.18.4.7681-7699
- Li, M. E., Yan, Y. W., Zhang, H. B., Jian, R. K., and Wang, Y. Z. (2020). "A facile and efficient flame-retardant and smoke-suppressant resin coating for expanded polystyrene foams," *Composites Part B: Engineering* 185, article 107797. DOI: 10.1016/j.compositesb.2020.107797
- Liu, L., Feng, J. B., Xue, Y. J., Chevali, V., Zhang, Y. B., Shi, Y. Q., Tang, L. C. and Song, P. G. (2023). "2D MXenes for fire retardancy and fire-warning applications: Promises and prospects," *Advanced Functional Materials* 33, article ID 2212124. DOI: 10.1002/adfm.202212124
- Lombardi, M., Fino, P., Malucelli, G., and Montanaro, L. (2012). "Exploring composites based on PPO blend as ablative thermal protection systems Part I: The role of layered fillers," *Composite Structures* 94, 1067-1074. DOI: 10.1016/j.compstruct.2011.10.019

- Mao, Y. Y., Wang, D., Hu, J. L., and Fu, S. H. (2023). "Mechanically flexible and flame retardant polyphenol-bridged casein/MXene composite for fire proofing repeatable contact/non-contact fire monitoring," *Chemical Engineering Journal* 454, article 140161. DOI: 10.1016/j.cej.2022.140161
- Sang, B., Li, Z. W., Li, X. H., Yu, L. G., and Zhang, Z. J. (2016). "Graphene-based flame retardants: A review," *Journal of Materials Science* 51, 8271-8295. DOI: 10.1007/s10853-016-0124-0
- Sartore, L., Penco, M., Sciucca, S. D., Mendichi, R., Landro, L. D., and D'Antone, S. (2006). "PPO-PC block-copolymers used as compatibilizers in PS/PC blends," *Journal of Applied Polymer Science* 100, 4654-4660. DOI: 10.1002/app.23208
- Severo, L. S., Rodrigues, J. B., Campanelli, D. A., Pereira, V. M., Menezes, J. W., de Menezes, E. W., Valsecchi, C., Vasconcellos, M. A. Z., and Armas, L. E. G. (2021). "Synthesis and Raman characterization of wood sawdust ash, and wood sawdust ashderived graphene," *Diamond and Related Materials* 117, article ID 108496. DOI: 10.1016/j.diamond.2021.108496
- Tian, A.X., Zhang, J. L., and Wang, Y. (2024). "Miscibility, thermal, and mechanical properties of recycled waste tire rubber-modified polystyrene sustainable composites," *BioResources* 20(1), 1273-1285. DOI: 10.15376/biores.20.1.1273-1285
- Tuan, V. M., Dat, N. H., Huynh, M. D., Trung, T. H., Cong, D. V., Thai, N. T., Long, P. T., Hai, L. N., Thang, D. X., and Giang, N. V. (2024). "Morphology, mechanical performance and fame resistance of acrylonitrile butadiene styrene (ABS)/ polyphenylene oxide (PPO) blends incorporated with halloysite nanoclay and polyphenylene ether-grafted maleic anhydride," *Polymer Bulletins* 81, 8083-8103. DOI: 10.1007/s00289-023-05090-z
- Vandi, L. J., Chan, C. W., Werker, A., Richardson, D., Laycock, B., and Pratt, S. (2018). "Wood-PHA composites: Mapping opportunities," *Polymers* 10(7), article 751. DOI: 10.3390/polym10070751
- Wiśniewska, P., Wójcik, N. A., Ryl, J., Bogdanowicz, R., Vahabi, H., Formela, K., and Saeb, M. R. (2023). "Rubber wastes recycling for developing advanced polymer composites: A warm handshake with sustainability," *Journal of Cleaner Production* 427, article 139010. DOI: 10.1016/j.jclepro.2023.139010
- Wiśniewska, P., W'ojcik, N. A., Kosmelaa, P., Ryl, J., Bogdanowicz, R., Vahabie, H., Shadmanf, A., Formela, K., and Saeb, M. R. (2024). "Recycled rubber wastes-based polymer composites with flame retardancy and electrical conductivity: Rational design, modeling and optimization," *Composites Science and Technology* 251, article 110563. DOI: 10.1016/j.compscitech.2024.110563
- Zhang, J. L., Wu, Q. L., Li, G. Y., Li, M. C., Sun, X. X., and Ring, D. (2017). "Synergistic influence of halogenated flame retardants and nanoclay on flame performance of high density polyethylene and wood flour composites," *RSC advances* 7, 24895-24902. DOI: 10.1039/C7RA03327C
- Zhang, J. L., De Hoop, C. F., and Wu, Q. L. (2024). "Environmentally friendly, low thermal conductivity, fire retarding, mechanically robust cellulose nanofibril aerogels and their use for early fire alarm sensors in thermally insulating sustainable building applications," *BioResources* 19(1), 15-18. DOI: 10.15376/biores.19.1.15-18

Zhang, J., Wang, Q. H., Xue, X. L., Li, M., Sun, X. W., Zhao, J. Q., Zhang, W., and Lu, C. H. (2023). "Waste flame-retardant polyurethane foam/ground tire rubber/carbon nanotubes composites with hierarchical segregated structures for high efficiency electromagnetic interference shielding," *Composites Part A: Applied Science and Manufacturing* 169, article 107530. DOI: 10.1016/j.compositesa.2023.107530

Article submitted: March 7, 2025; Peer review completed: May 10, 2025; Revised version received and accepted: July 21, 2025; Published: July 29, 2025. DOI: 10.15376/biores.20.3.7713-7727

#### **APPENDIX**

The TG-FTIR spectra of WTRPS and WTRPS/P40/M15 composites are shown in **Fig. S1**. WTRPS and WTRPS/P40/M15 composites showed almost similar profiles, indicating that the thermal degradation mechanism did not change with the addition of PPO and MXene. The intensity reduction of characteristic peaks (*e.g.*, 694 cm<sup>-1</sup> as C-H benzene ring at 430 °C) supported the enhanced fire retardancy of WTRPS/P40/M15 composites.

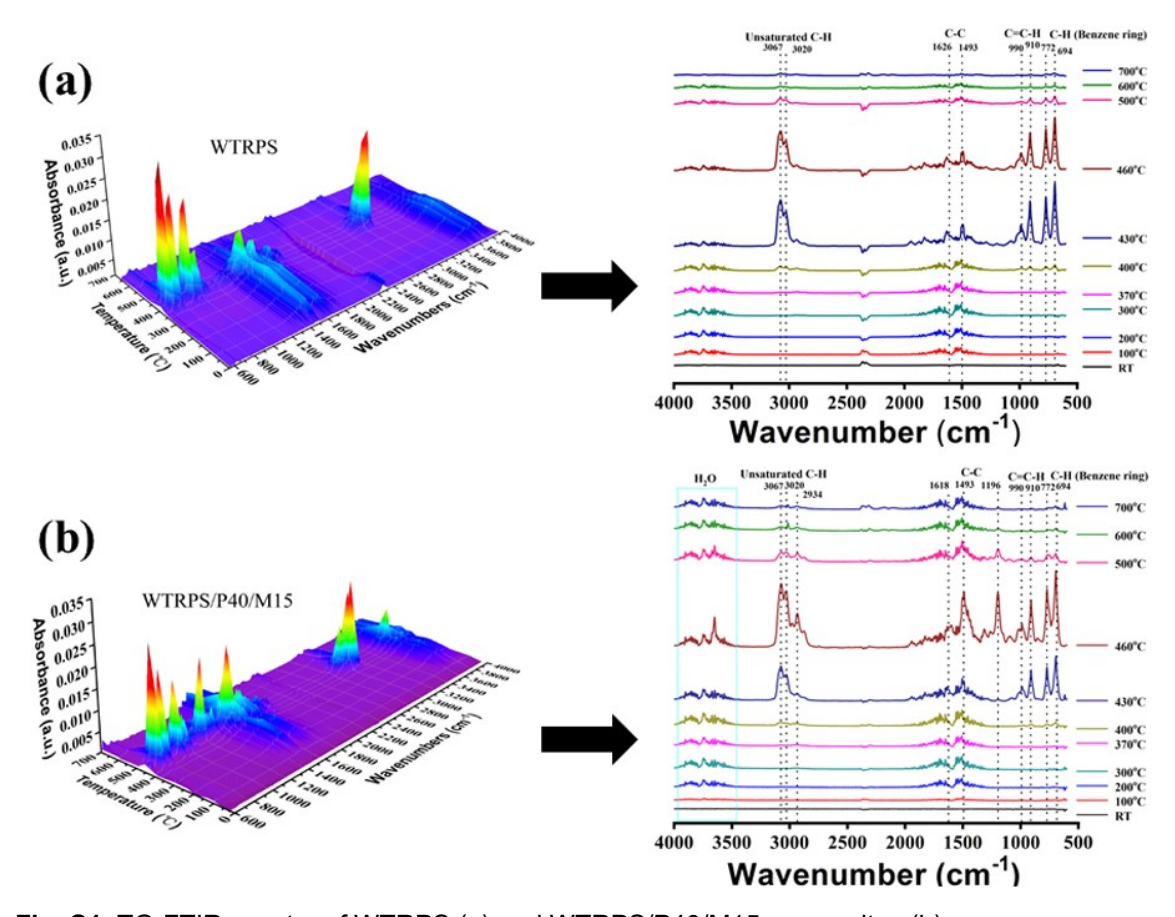


Fig. S1. TG-FTIR spectra of WTRPS (a) and WTRPS/P40/M15 composites (b)